Chapter 13

Stationary and Progressive Waves in Rings and Hollow Cylinders[1]

13.1. Introduction

The objective of this chapter is to show that in some circumstances, experimenters do not have material samples at their disposal which are made according to the recommendations of national standards' offices. In such situations, the samples tend to be fabricated from an existing mechanical object, such as a hollow cylinder, curved rod, etc. The nature of the material is often unknown; and experimenters must choose the shape and number of samples based on the following considerations:

(i) whether it is an isotropic or anisotropic material;

(ii) the shape of the sample to be fabricated from the existing object and whose elastic (or viscoelastic) characteristics are to be evaluated;

(iii) the choice of special set-ups, which depends on the samples and their unusual shapes.

With regard to the first item, the problem is to evaluate the symmetry directions of the existing object. Often, fabrication techniques furnish information concerning the symmetry of an anisotropic material.

Chapter written by Yvon CHEVALIER and Jean Tuong VINH

1 This chapter contains long extracts from J.P. Bersegol's final report submitted to obtain a mechanical engineering diploma [BER 77].

Mechanical Characterization of Materials and Wave Dispersion: Instrumentation and Experiment Interpretation
Edited by Yvon Chevalier and Jean Tuong Vinh

This consideration has been discussed in detail elsewhere (see Chapter 1 [CHE 10]). The number of elastic (or viscoelastic) constants depends on the symmetry degree of the material.

For item (ii) above, the choice of the sample geometry is restricted to the object's symmetry itself. Appropriate equations of motion have to be written as well as appropriate boundary conditions. For item (iii), special sample holders need to be designed.

Initially, in our research, the vibrations of rings and hollow cylinders were realized in the framework of an industrial contract. The object was to estimate the elastic moduli of pyrolytic graphite used in the electronics industry.

13.2. Choosing the samples based on material symmetry

The fabrication technique might serve as a guide to the symmetry degree of the material. If the hypothesis of a material symmetry axis of the object is adopted, a transverse isotropic material is the first one. Figure 13.1 shows a hollow cylinder with three possible samples. Rod (A), whose axis is collinear with the cylinder axis oz, has a curved cross-section. Ring (B) maintains the symmetry of the cylinder. The whole object (C) can be used for torsion tests. A curved rod, not represented in Figure 13.1, which makes an angle Θ with respect to the z axis of the object, can be used to evaluate Poisson's ratio ν_{rz}.

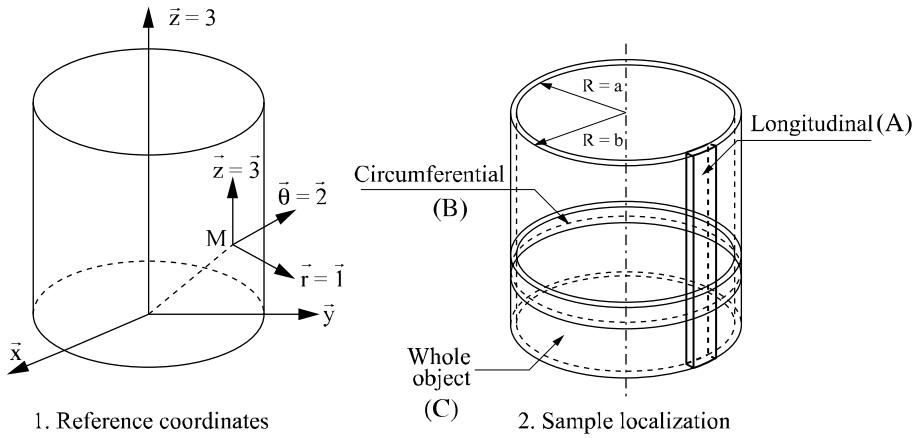

Figure 13.1. *Initial object from which samples are to be cut (1); cylindrical coordinates are used for the geometry of the object (2) three kinds of samples are cut from the object: A: longitudinal rod; B: a ring (circumferential); C: the whole object*

Sample and moduli	Equations of motions	Remarks
(1) E_z, $G_{z\theta} = G_{zr}$	Bernoulli-Euler's or Timoshenko's equation or Saint Venant's equation	Inertia moment of the cross-section to be evaluated
(2) E_r	Flexural ring equation of motion (Appendix 13A)	More convenient to handle than curved rod
(3) $\nu_{rz} = \nu_{zr}$	Coupled equations of motion (torsional-bending) to be written	Warping phenomenon

Table 13.1. *Three samples cut from hollow cylinder to be used in bending and torsional tests*

Table 13.1 contains comments concerning the three samples. with the exception of sample 3, whose coupled equations of motion are difficult to handle, the two first samples (1 and 2) allow only three elastic moduli to be evaluated. The two remaining elastic moduli necessitate wave propagation through the sample thickness. Low frequency vibrations are consequently not appropriate. Ultrasonic waves are referred to and are easier to use[2]. The fourth sample is the whole hollow cylinder itself. Torsional vibration tests enable $G_{\theta z}$ to be evaluated.

13.2.1. *Ultrasonic tests*

Ultrasonic tests are applicable if the thickness of the hollow cylinder is not too small (i.e. if the thickness is at least three or four times the wavelength). They are useful for shear modulus evaluation.

13.3. Practical realization of a special elasticimeter for curved beams and rings: in plane bending vibrations

As we have to deal with curved beams and rings, elasticimeters need to be specially conceived and realized, in which the sample holder must be well adapted to the sample geometry, on the one hand, and able to satisfy the specific boundary considerations, on the other hand.

2 Ultrasonic measurements enable the stiffness matrix coefficients C_{ijkl} to be evaluated when vibration tests give compliance matrix coefficients S_{ikjl} from which elastic moduli are deduced. As we have to deal with pyrolytic graphite, which is weakly viscoelastic, the hypothesis of predominant elastic behavior permits us to use low frequency vibration techniques and ultrasonic waves (at high frequency) concurrently. If this hypothesis is not valid, tests of the same family (vibrations of rod, ring and cylinder) or ultrasonic progressive waves should be chosen.

13.3.1. *Clamping of the ring sample*

Taking into account the symmetry of the sample, a clamping system with two rigid cylinders is adopted here (see Chapter 3, section 3.5). Figure 13.2 shows the sample holder which is easy to realize. Details of double clamping techniques, to obtain symmetric clamping with respect to the symmetry of the ring, can be found in Chapter 3.

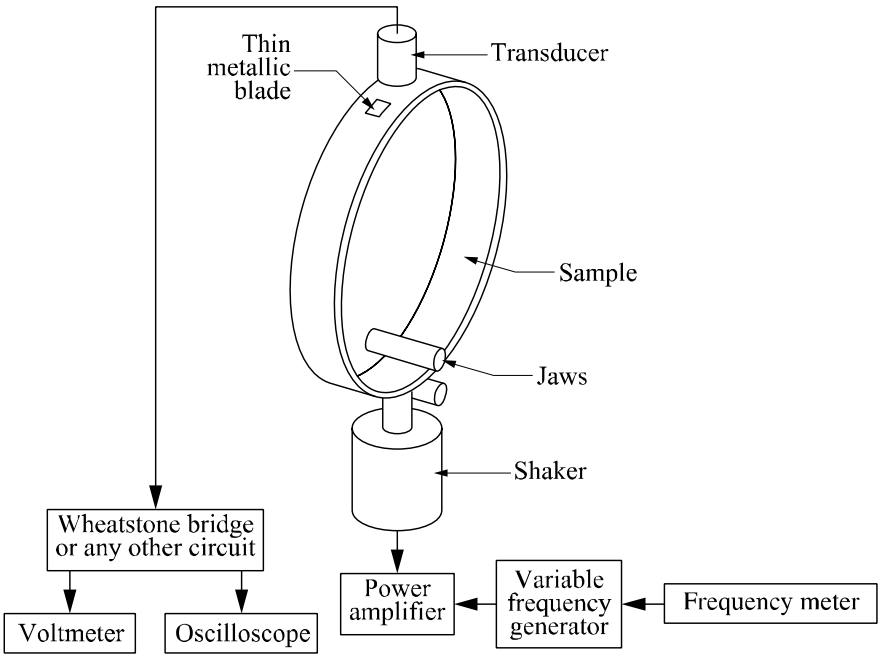

Figure 13.2. *Electronic set-up. Precautions must be taken to prevent damage to the moving coil of the shaker from the sample weight and its holder. The ring is submitted to bending vibrations. The sample holder is realized by double pseudo-clamping. In this figure, the mechanical system to apply to both cylinders and uniform pressure are not represented*

13.3.2. *Electromechanical shaker (see also Chapter 4)*

An electromechanical shaker is used when mechanical excitation is realized by means of short rigid rods fixed to the sample holder. The electric power of the shaker must be sufficient to deliver alternative motion to the sample via the holder. The weight of the set (sample and sample holder) is taken into account for the moving coil of the shaker so as to avoid its deterioration. Finally, the mechanical

rigidity of the moving coil is set in parallel with an external spring made from a blade attached at both sides of the moving coil.

13.3.3. *Transducers*

To avoid the additional weight of a transducer fixed or glued to the sample (an accelerometer, for example) a contactless displacement transducer is adopted. On the upper side of the ring, only a small, thin, light, steel blade is glued to the ring.

If the transducer response is non-linear, a linearizing electronic circuit must be used. It is possible to use a couple of inductive transducers fixed on both sides of the ring on a rigid bar to obtain a better linear transducer response (see Chapter 5).

13.3.4. *Wheatstone bridge (or other signal conditioner)*

If inductive contactless transducers are used, an alternative current Wheatstone bridge is used. The main precaution is to choose a carrier frequency f_{osc} (for the oscillator feeding the bridge), that is high enough so that $f_{osc} \geq 5$ to 10 f_h, where f_h designates the highest measured frequency. Often, a low pass filter is disposed at the output of the bridge. In that case, the cut-off frequency of the filter is considered to be the upper bound of f_h.

13.3.5. *Variable frequency generator and frequencymeter*

They are used to measure the forced oscillation frequency. At high frequency, forced excitation can produce a high structural mode with nodes on the ring. Localization of these vibration nodes is not necessary.

13.3.6. *Torsional vibration of a hollow cylinder*

Figure 13.3 shows the three possible set-ups. Figure 13.3(a) corresponds to the application of a torque on the upper disk, the lower disk being fixed. In Figure 13.3(b), displacement is imposed on the lower disk. Figure 13.3(c) shows a torque applied to the lower disk. This last solution is retained for torsion tests.

In Figure 13.4, adjustable weights are symmetrically fixed on the higher disk. Figures 13.3 (a), (b) and (c) represent the tests used to obtain the circumferential Young's modulus $E_{\theta\theta}$ and shear modulus $G_{\theta z}$, respectively.

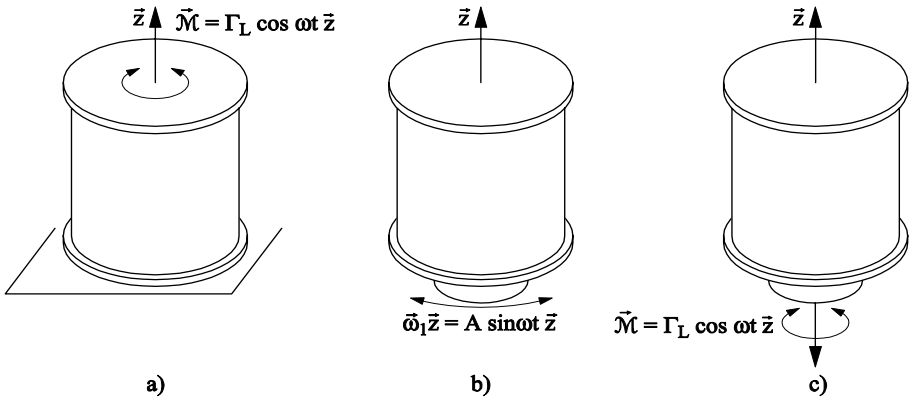

Figure 13.3. *The three possible excitations applied to the hollow cylinder: (a) torsional couple applied to the upper disk, the lower disk being fixed; (b) forced displacement imposed on the lower disk, the upper cylinder being free; (c) torque imposed on the lower disk*

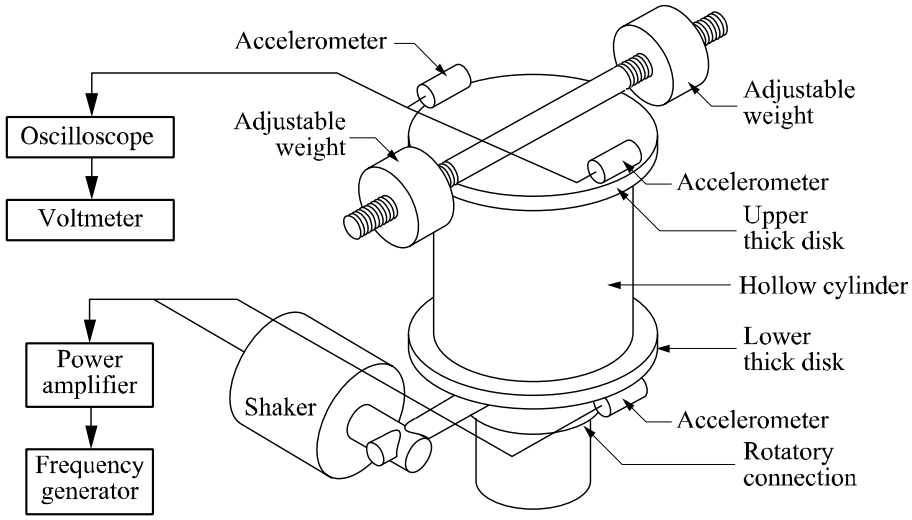

Figure 13.4. *Schematic representation of torsion test on a hollow cylinder*

Figure 13.5(a) shows the torsional test. The sample cross-section is curved and cut from a hollow cylinder of the same thickness. Figure 13.5(b) corresponds to bending tests.

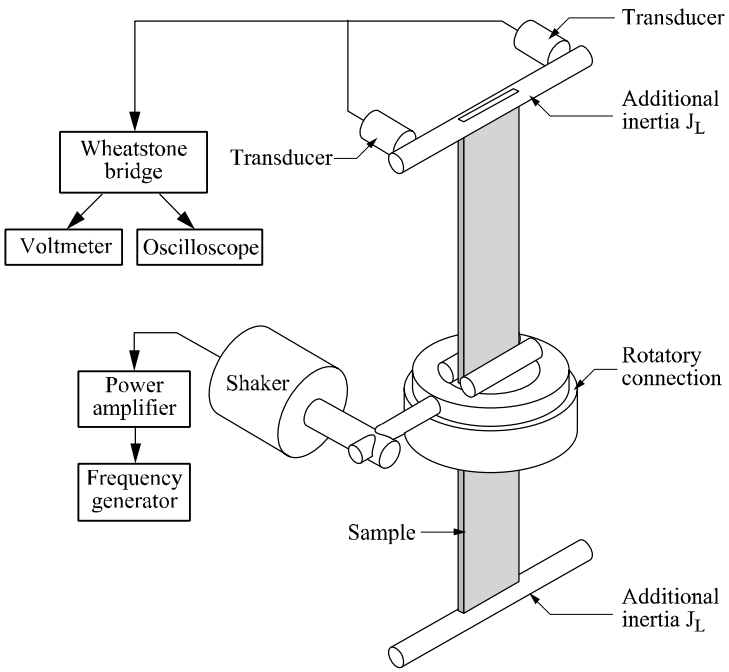

Figure 13.5(a). *Mechanical set-up for torsional test on rod with curved cross-section*

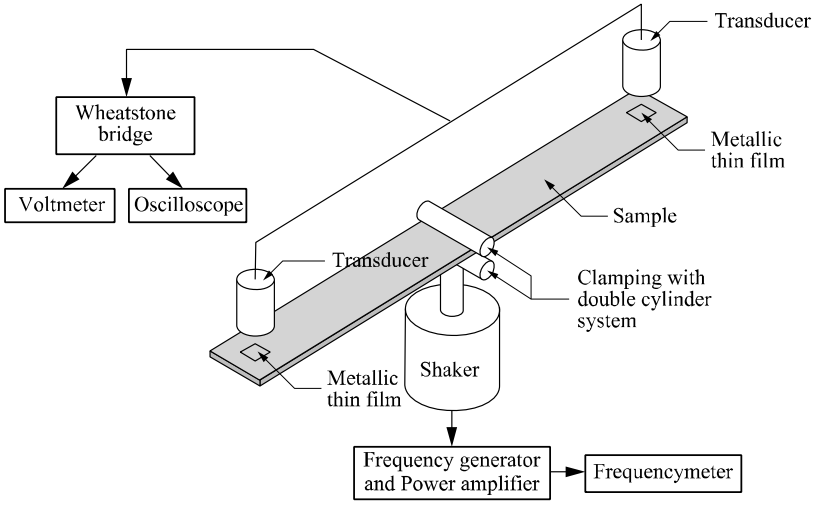

Figure 13.5(b). *Bending test on rod with curved cross-section. Instrumentation is similar to that used for the torsional test in Figure 13.5(a)*

13.4. Ultrasonic benches

Ultrasonic benches can be used to estimate coefficients of the material stiffness 6x6 matrix {C}. Remember that ultrasonic tests do not enable us to directly evaluate elastic moduli which are deduced from coefficients of compliance 6x6 matrix {S}. If ultrasonic waves are used to complete the missing information for {S}, shear waves are used to evaluate the shear modulus, which does not necessitate the matrix inversion applied to the stiffness matrix (see Chapter 1 [CHE 10]).

13.4.1. *Direct contact benches with two identical transducers*

One transducer serves as emitter, the other as receiver. The basic theory of ultrasonic wave propagation is presented elsewhere (see Chapter 10 [CHE 10]). Practical information about ultrasonic benches is presented here.

Figure 13.6 shows a direct contact bench for shear waves. It is necessary to adjust the wave polarization of both transducers by means of a goniometer. Translational micrometers are used to adjust the transmitter axis with respect to the receiver axis. For longitudinal waves, a direct contact bench is presented in Figure 13.7. The adjustments of the two transducer axes are similar to those used in Figure 13.6 for shear waves , the wave polarization of longitudinal waves being collinear with the direction of wave propagation.

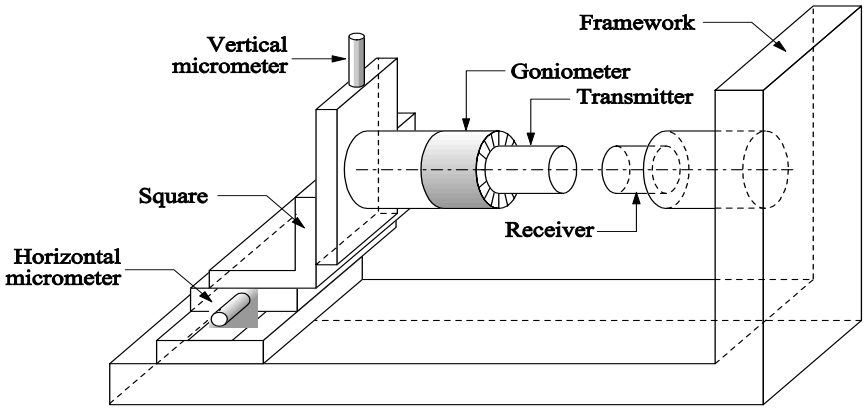

Figure 13.6. *Ultrasonic direct contact bench for shear waves. The sample is held between two transducers, one used as transmitter, the other as receiver. The polarization wave direction of the transmitter is adjusted by a goniometer. Two sliding caliper gauges with linear micrometers (one horizontal and one vertical) are used to adjust the transmitter position with respect to the receiver position*

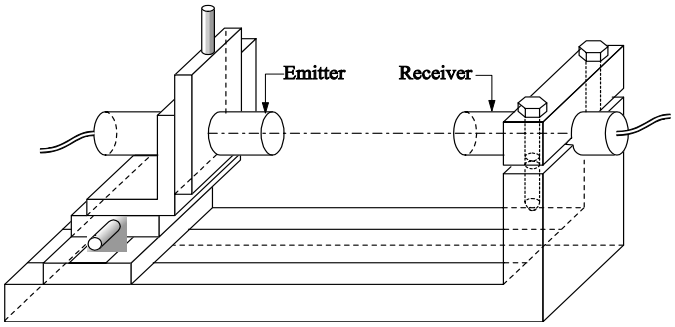

Figure 13.7. *Ultrasonic direct contact bench for longitudinal waves. Three coordinate axis adjustments are necessary for the transmitter. Rotary adjustment is not necessary, unlike in Figure 13.6, polarization vector is collinear with propagation direction vector. The oblique incidence of ultrasonic waves is obtained with a special ultrasonic lens*

In principle, the measurements can be made without the benches presented in Figures 13.6 and 13.7. However, it is difficult to adjust the coincidence of both transducer axes, on the one hand, and the coincidence of the same wave polarization of the transducers for shear wave, on the other hand.

13.5. Experimental results and interpretation

13.5.1. *Bending tests and Young's modulus E_z estimation*

The sample is presented in Figure 13.8.

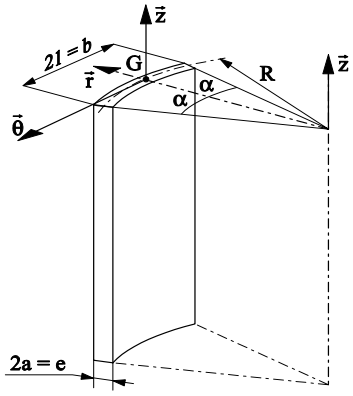

Figure 13.8. *Sample with curved cross-section. Angle 2α is defined at the z axis of the hollow cylinder*

The equation of motion is presented in Appendix 13B. The only difference with classical bending tests for a straight rod with rectangular cross-section resides in the curved cross-section which requires calculation of the inertia moment with respect to the gravity center G of the cross-section.

13.5.1.1. *Calculation of OG (O being the trace*[3] *of the cylinder axis)*

By definition, using Cartesian coordinates (x,y,z):

$$OG = \frac{\iint_D y dx dy}{\int_D dx dy} \quad [13.1]$$

With cylindrical coordinates (ρ,θ,z), from tests undertaken as shown in Figure 13.8:

$$\frac{\int_{-\alpha}^{+\alpha}\int_{R-a}^{R+a} \rho^2 \cos\theta \, d\rho \, d\theta}{\int_{-\alpha}^{+\alpha}\int_{R-a}^{R+a} \rho \, d\rho \, d\theta} = \frac{\sin\alpha}{R\alpha}\left[R^2 + \frac{a^2}{3}\right] \quad [13.2]$$

13.5.1.2. *Inertia moment in Cartesian coordinates (Figure 13.8)*

$$I_{o\theta} = \iint_D y^2 dx dy \quad [13.3]$$

In the cylindrical coordinates:

$$I_{o\theta} = \iint_D \rho^3 \cos^2\theta \, d\rho d\theta$$

$$= \int_{R-\alpha}^{R+\alpha} \rho^3 d\rho \int_{-\infty}^{+\infty} \cos^2\theta \, d\theta \quad [13.4]$$

$$I_{o\theta} = 2Ra(R^2 + a^2)\left(\frac{\sin 2\alpha}{2} + \alpha\right) \quad [13.5]$$

3 The projection of the axis on a transverse section of the cylinder.

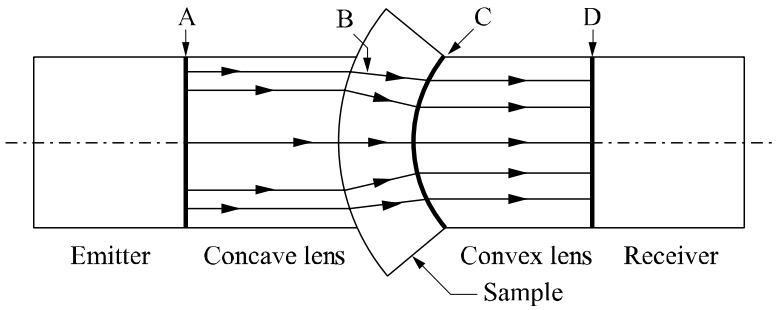

Figure 13.9. *Two ultrasonic lens are used to focus an ultrasonic beam on the sample and the receiver. A, B, C, and D represent thin layers of coupling liquid which are necessary. For a shear wave, the coupling liquid must be viscous*

This inertia with respect to O must be converted into $I_{G\Theta}$ with G the center of gravity previously evaluated. Huygen's theorem is used. If S is the cross-section area, and d_G the distance between O and G, then:

$$I_{G\theta} = I_{OG} - S d_G^2 \qquad [13.6]$$

$$= I_{G\theta} = 2a\,R\left[(R^2+a^2)\left(\frac{\sin 2\alpha}{2}+\alpha\right) - \frac{2\sin^2\alpha}{R^2\alpha}\left(R^2+\frac{a^2}{3}\right)^2\right] \qquad [13.7]$$

[13.7] can be expressed versus l as:

$l = R\alpha$, $R = l/\alpha$

$$I_{G\theta} = 2a\left[\frac{l^3}{\alpha^4}\left(\alpha^2 + \frac{\alpha}{2}\sin 2\alpha - 2\sin^2\alpha\right) + \frac{la^2}{\alpha}\left(\frac{\sin 2\alpha}{2}+\alpha\right) - \frac{4la^2}{3\alpha^2}\sin^2\alpha - \frac{2a^4}{91}\sin^2\alpha\right] \qquad [13.8]$$

If the angle α is small, a limited series expansion can be effected, as follows:

$$I_{G\theta_C} \cong I_{G\theta_{rect}}\ (1+\epsilon) \qquad [13.9]$$

The first term designates the inertia moment corresponding to the curved cross-section, the second term designates the inertia moment for the rectangular cross-section, with thickness h and width b.

$$\left[1 + I_{G\theta_C}\right] \cong \frac{be^3}{12}\left[1+\varepsilon\right] = \frac{4\ell\, a^3}{3}\left[1+\varepsilon\right] \qquad [13.10a]$$

$$\epsilon \cong \frac{\alpha^2}{3la^2}\left[\left(\frac{l^3}{5} - \frac{a^4}{l} + la^2\right) - \frac{2l^3}{35}\alpha^2\right] \qquad [13.10b]$$

If Bernoulli-Euler's equation of motion is used (see Chapter 10 in [CHE 10]), the Young's modulus is given by:

$$E = \frac{\rho S \omega^2 L^4}{I_{G\theta_C}\beta^4} \qquad [13.10c]$$

where β depends on the eigenmode rank related to the boundary conditions of the rod sample; see, equation [13.C.4]. For the clamped-free rod, the first values of β are:

$$\beta_1 = 1.875104,\ \beta_2 = 4.69409,\ \beta_3 = 7.855,\ \beta_4 = 10.996,\ \beta_n = (2n-1)\pi/2$$

$$\text{with } n > 4 \qquad [13.10d]$$

When using [13.10c] one must ensure that inertia and shear effects can be neglected.

13.5.1.3. *Experimental results*

The set-up in Figure 13.5(b) is used:

M: half sample weight = 2.47×10^{-3} kg.

b width = 1.01×10^{-2} m, h thickness = 10^{-3} m.

L half length[4] = 15.07×10^{-2} m (the symmetry of the sample is respected, pseudo clamping is applied at the sample middle).

R radius of curvature = 5.52×10^{-2} m.

ε (equation [13.10a]) = 5.961×10^{-2}.

f (resonance frequency) = 120.9 Hz.

E_z (Young's modulus) = 2.765×10^{10} Pascal.

4 Half weight and half length are used to take the symmetry (with respect of the center of the rod which is submitted to force vibration) into account.

13.5.2. *Shear modulus estimation by torsional tests effected on a rod sample*

The theory of torsional vibration is presented elsewhere (see Chapter 5 [CHE 10]). The experimental set-up is presented in Figure 13.5(a). The same sample used in the bending test presented above is adopted here.

13.5.2.1. *Elementary Saint Venant's equation of torsion*

The elementary Saint Venant's equation of torsion is used here as a first approximation. The second order equation of motion is used:

$$\rho\, I_p \frac{\partial^2 \theta}{\partial t^2} = C_T \frac{\partial^2 \theta}{\partial z^2} \qquad [13.11a]$$

$$\text{with } I_p = \iint_D (x^2 + y^2)\, dx\, dy \qquad [13.11b]$$

where ρ is density, I_p polar inertia of the cross-section, C_T torsional stiffness and θ torsion angle.

13.5.2.2. *Eigenvalue equation*

The eigenvalue equation is given by:

$$\frac{\rho L I_p}{J_L} = \zeta \tan \zeta \qquad [13.11c]$$

Remember that ζ is adopted in the expression of torsion angle $\theta(z,t)$ for $z = L$ (half sample length):

$$\theta(L,t) = e^{j\omega t}\left[A \cos \frac{\zeta z}{L} + B \sin \frac{\zeta z}{L}\right] \qquad [13.11d]$$

where J_L designates additional inertia (see Figure 13.5(a)). In Equation [13.11c] presented above, the first member is known. This equation has to be solved to obtain the first root ζ :

$$\frac{\rho L I_p}{J_L} = \gamma = \frac{M}{24 J_L}(b^2 + e^2) \cong \zeta^2 \qquad [13.11e]$$

As γ is small (of the order 3 x 10^{-3}), a series expansion limited to the fourth order gives:

$$\zeta_1^2 \cong \frac{1+\sqrt{1+4/3\gamma}}{2/3} \qquad [13.11f]$$

13.5.2.3. *Torsion stiffness*

Bringing [13.11d] to [13.11a] we obtain:-

$$C_T = LJ_L\omega^2 \frac{\tan\ \zeta}{\zeta} \qquad [13.12]$$

13.5.2.4. *Shear modulus G_{rz}.*

The shear modulus is deduced from the torsion stiffness expression (see Chapter 10, in [CHE 10]):

$$C_T = G_{\theta z}\, hb^3\, \beta_T(c) = G_{rz}\, bh^3\, \beta_T(1/c) \qquad [13.13]$$

In this equation, warping of the section is represented by the factor $\beta_T(c)$ which is expressed by a series:

$$\beta_T(c) = [\ \frac{1}{3} -.\ \frac{64}{c\pi^5}\sum_{k=1,3,5\ldots}\ \frac{1}{k^5}\ \tanh\frac{k\pi c}{2}\ ] \qquad [13.14]$$

and c is defined as:

$$c=\frac{\mu e(thickness)}{b(width)} = \frac{e}{b}\sqrt{\frac{G_{\theta z}}{G_{rz}}} \qquad [13.15]$$

As the material is supposed to be transverse isotropic with material symmetry collinear with the z axis: $G_{rz} = G_{\Theta z}$. [13.15] is then reduced to

$$c'=1/c = \frac{e}{b} \qquad [13.16]$$

From [13.15] and [13.13] we can write:

$$\frac{C_T}{bh^3\beta(\frac{1}{c})} \qquad [13.17]$$

$$G_{rz} = \frac{C_T}{be^3\beta_T(c')}$$

$\beta_T(c)$ can be estimated either directly from [13.14][5] or from a table with possible interpolation.

13.5.2.4.1. Experimental results

L (half length) = 13.8 x 10^{-2} m

b (width) = 1.01 x 10^{-2} m

e (thickness) = 10^{-3} m

M (half weight) = 2.212 x 10^{-3} kg

J (additional rotational inertia) = 3.084 x 10^{-6} m.kg

I_{Gz} (quadratic moment) = 8.67 x 10^{-11} m^2.kg

γ (equation [13.11e]) = 3.08 x 10^{-3}

ζ^2 (equation [13.11c]) = 3.076 x 10^{-3}

$\beta_T(c')$ (equation[13.14]) = 0.292

c' (equation [13.16]) = b/ h = 5.1

f (resonance frequency) = 66.2 Hz

$G_{rz} = C_{44} = 3.179 \times 10^9$ Pascal = $G_{\Theta z}$

13.5.2.5. *Remarks concerning torsion test with a straight sample*

This was not a straight sample with a rectangular cross-section. The cross-section is curved and the torsion center is not coincident with the gravity center. The sample was subjected to coupled motions (bending and torsion) and, during the test, bending motion was neglected.

---

5 As the series in [13.14] is quickly convergent, three or four terms are sufficient in a usual application. However, as c in this peculiar application is high $c' > 5$, β reaches nearly a horizontal asymptote. A numerical computation is then necessary.

The accuracy of β_T depends on the value c'. As c' = 5.1, the curve β_T versus c reaches nearly an asymptotic value and an error on the adopted c' value has a strong influence on β_T. Consequently β should be evaluated numerically with accuracy.

The hypothesis of transverse isotropy of the material is to be checked with further experimental results to validate (or invalidate) this hypothesis. Additional tests are consequently necessary to improve the estimation of elastic moduli.

13.5.3. *Bending tests on ring*

The experimental set-up is presented in Figure 13.2. Equations of motion are briefly presented in Appendix 13A devoted to bending vibration of a ring. The expression of Young's modulus E_Θ is given by formula, in Appendix 13B, which is also presented here:

$$E_\Theta = \frac{4\pi^2}{Q_k I}\rho S R^4 = \frac{2\pi f_k^2}{Q_k I} M R^3 \qquad [13.18]$$

where Q_k is the root of order k obtained by solving the third order characteristic equation. The three values of Q_k (k= 1; 2 ,3) are given by [CHE 10] equation [9.39] or [13.A.3]:

$[Q_1=2.56, \quad Q_2=33.15 , \quad Q_3=147.3]$

The parameter values in [13.18] are indicated below:

M (ring weight) = 6.63×10^{-3} kg

R (medium radius) = 5.5×10^{-2} m

b (width) = 10.3×10^{-3} m

e (thickness) = 10^{-3} m

f_k (with k=1) (first eigenfrequency) = 96 Hz

$E_\Theta = 2.9 \times 10^{10}$ Pascal

13.5.4. *Torsion tests on a hollow cylinder*

This test enables shear modulus $G_{\Theta z}$ to be estimated (Figure 13.4). Two kinds of test are adopted. The first corresponds to the sample presented in Figure 13.3(c) in which the upper plate has no additional weight, as in Figure 13.4. The second test concerns the sample with additional and adjustable weights presented in Figure 13.4.

13.5.4.1. *Upper disk without additional weight*

Appendix 13B presents an experimental method of evaluation of inertia moment by a pendulum suspended by three threads.

The additional inertia is $J = 2.36528 \times 10^{-3}\ m^2\ kg$.

It is shown that at resonance, the following equation must be satisfied:

$$G_{\Theta z} . K \beta_0 \cos \beta_0 L = J\omega^2 \sin \beta_0 L \qquad [13.19]$$

with $\beta_0 = \frac{\zeta}{L}$

$$\beta_0 = \omega \sqrt{\frac{\rho}{G_{\theta z}}} ; \quad \omega^2 = \frac{\beta_0^2}{\rho} G_{\theta z} \qquad [13.20]$$

Eigenvalue equation is:

$$\frac{\rho K L}{J} = \beta_0 L \tan (\beta_0 L) \qquad [13.21]$$

That is a classical elementary equation of torsional motion with additional inertia moment J at one end:

$$\rho K L = J_c = \frac{4\rho L(b^4 - a^4)\pi}{2} \qquad [13.22]$$

where b is the external curvature radius and a the internal curvature radius, thickness e=b-a, That is the inertia moment of the cylinder with respect to axis $O\vec{z}$. Then the eigenvalue equation is:

$$\frac{J_c}{J} = \zeta_k \tan \zeta_k \quad [13.23]$$

$$G_{\Theta Z} = \rho\omega^2/\beta_0^2 = \rho\omega k^2 L^2/ \zeta_k^2 = 4\pi^2 \rho L^2 f^2_k / \zeta_k^2 \quad [13.24]$$

For the hollow cylinder

$$J_C = M(b^2+a^2) / 2 = M (4R^2 + e^2) / 4 \quad [13.25]$$

13.5.4.1.1. Experimental results

M = M_C (cylinder weight) = 96.10^{-3} kg

R (curvature radius) = $5.52.10^{-2}$ m

h (thickness) = 10^{-3} m

L (length) = 138 x 10^{-3} m

J_C (quadratic moment) = 2.9254 x 10^{-4} m^4

J (inertia of the upper disk) = 2.36 x 10^{-3} m^2.kg

f (frequency) = 1,108 Hz

$G_{\Theta z} = C_{44}$ = 1.414 x 10^{10} Pascal

13.5.4.2. *Upper disk with additional weight*

Figure 13.4 shows additional weights and their distance from the cylinder axis, the upper disk inertia being much greater than the additional weight inertia. The shear modulus $G_{\Theta z}$ is given by:

$$G_{\Theta z} = \frac{K\Delta J f_1^2 f_2^2}{f_1^2 - f_2^2} \quad [13.26]$$

$$K = \frac{8\pi L}{eR(4R^2 - e^2)} \quad [13.27]$$

$\Delta J = J_1 - J_2$

where $\Delta J = m (d_1^2 - d_2^2)$; m additional weight, and d distances of additional weight to the cylinder axis.

13.5.4.2.1. Experimental results

K (equation [13.27]) = 5.017×10^6

Δ J (inertia variation) = 2.742×10^{-3} m^2.kg

f_1 (first resonance frequency) = 627 Hz

$C_{44} = G_{\Theta z} = 1.336 \times 10^{10}$ Pascal

13.5.4.3. *Comments*

The method using additional weights is the simplest method to evaluate the inertia of a mechanical system which can have a complicated geometry. It does not necessitate knowing the value of upper disk inertia which is tedious to evaluate.

Adjustment of the distance of the additional weights with respect to the cylinder axis must be carefully effected.

Additional weights must be maintained firmly in position when experimental tests are carried out.

13.5.5. *Ultrasonic tests*

13.5.5.1. *Interest of ultrasonic tests and their limitation-*

Among the various methods presented in this book, ultrasonic methods are the easiest to carry out and handle. Results can be rapidly obtained even with small samples. However, there is a problem we must consider before using this technique.

If the material is strongly viscoelastic, the complex viscoelastic stiffness matrix coefficients are frequency dependent and the ultrasonic working frequency is much higher than the acoustic vibration frequency of the rod or sample used in this chapter.

In this condition, it is difficult to compare results obtained by vibration techniques with results deduced from ultrasonic tests. This is the case of some polymers and rubbers, etc.

However, if ultrasonic waves propagate in such viscoelastic mediums without dispersion and high attenuation, such a technique might be used to check the degree of symmetry of the material.

If the material is weakly viscoelastic with low damping capacities, ultrasonic methods can be used to obtain complementary results to those furnished by vibration tests. This is the case of special composites fabricated with high strength long fibers (graphite, boron, etc.) and a high polymer as matrix.

High performance composites such as a three-dimensional graphite composite have viscoelastic moduli which vary weakly with frequency. An ultrasonic method can then be used.

The material under test in this chapter is pyrolytic graphite. Ultrasonic tests can be used concurrently with other test methods to estimate elastic coefficients. Remember that ultrasonic tests using progressive waves permit the coefficients of 6x6 stiffness matrix {C} to be obtained when vibration tests allow evaluation of coefficients of compliance 6x6 matrix {S}. With the exception of shear moduli, it is difficult to obtain directly coefficients of {S} unless all the coefficients of {C} are evaluated. And then the inversion of matrix {C} allows matrix {S} to be obtained.

13.5.6. *Utilization of transmitted waves*

Tests with transmitted waves, which travel through a sample only once, give rise to simple methods. Figures 13.7 and 13.8 show how to realize the two corresponding benches.[6]

13.5.7. *Test procedure*

13.5.7.1. *Acoustical lens for curved plates*

In order to improve test accuracy, two acoustical lenses made from a high polymer such as polymethacrylate or plexiglas can be made (Figure 13.9).

They focus the ultrasonic beam which is nearly parallel when reaching the receiver. Coupling liquid layers are used as thin as possible so as to neglect their thickness with respect to the sample thickness. The part of the ultrasonic beam which reaches the receiver first corresponds to the sample thickness.

6 Details concerning the practical use of ultrasonic benches can be found in Chapter 4.

13.5.7.2. *Electronic set-up*

The electronic equipment required is reduced and outlined in basic form in Figure 13.10.

A tone burst signal with adjusted repetition rate is produced by an impulse generator with a power amplifier (output electric impedance, Zo ≅ 200 Ohms). The signal is applied to a transducer which is used as an emitter. The sweeping of an oscilloscope is triggered by the impulse generator. The signal from the receiver is analyzed on the oscilloscope screen.

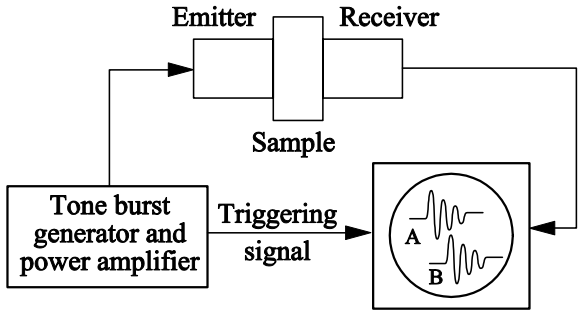

Figure 13.10. *Electronic equipment is reduced to its simplest expression*

Two measurements are made:

– one without a sample, Signal A, corresponding to the position of a signal received on the oscilloscope at position A;

– one with a sample, Signal B, corresponding to the position where the signal is visualized on the oscilloscope (position B) after travelling through the sample.

The time interval between oscilloscope measurements A and B corresponds to the travel time in the sample. This difference between the two positions A and B is the travel time in the sample: $\Delta t = t_B - t_A$ which can be accurately evaluated. The corresponding velocity is : $v_{i/j} = e / \Delta t$, where e is the sample thickness.

Subscripts $\vec{i}$ and $\vec{j}$ designate the wave polarization and propagation direction, respectively. If these directions are coincident, we have a pure longitudinal wave. If these directions are orthogonal, we have a pure shear wave. If these directions are neither collinear nor orthogonal we have coupled waves. This serves to evaluate a non diagonal stiffness coefficients of the {C} matrix.

13.5.8. *Some experimental results*

Table 13.2 gives the types of waves. Table 13.3 contains the three elastic coefficients.

Normal to phase plane	Propagation direction	Type of wave	Elastic coefficient
$n_1 = 1$, $n_2 = n_3 = 0$	1	L (longitudinal)	$C_{11} = C_{22} = \Gamma_{11} = \rho v^2$
$n_3 = 1$, $n_1 = n_2 = 0$	3	L(longitudinal)	$C_{33} = \Gamma_{33} = \rho v^2$
$n_3 = 1$, $n_2 = n_1 = 0$	2	T (transverse)	$C_{44} = \Gamma_{22} = \rho v^2$

Table 13.2. *Type of wave and corresponding elastic coefficient of stiffness matrix {C}*

Velocity and wave nature	Stiffness coefficient	Uncertainty
4,395m/**s**, longitudinal	$C_{11}=C_{22}= 3.090 \times 10^{10}$ Pa.	1.4%
2,270 m/s, longitudinal	$C_{33} = 0.825 \times 10^{10}$ Pa.	4%
1,157m/s, transverse	$C_{44}= C_{55}= 0.214 \times 10^{10}$Pa	3.5%

Table 13.3. *Ultrasonic measurements on pyrolytic graphite*

13.5.9. *Stiffness matrix {C} and compliance matrix {C} evaluated by ultrasonic methods*

If the transverse isotropy of the material needs to be checked, the non diagonal coefficient $C_{12} = C_{11} - 2C_{66}$ is given by transverse isotropy symmetry. By matrix inversion, we obtain:

$$C_{13} = C_{33} \frac{[\, C_{11}^2 - C_{12}^2 - E_1 C_{11} \,]}{4C_{66} - E_1}$$

$$E_1 = C_{33} - \frac{2C_{13}^2}{C_{11} + C_{12}}$$

$$\nu_{12} = \nu_{21} = \frac{C_{12}C_{33} - C_{13}^2}{C_{11}C_{33} - C_{13}^2}$$

$$\nu_{31} = \nu_{32} = \frac{C_{13}}{C_{11} + C_{12}}$$

$$\nu_{13} = \nu_{23} = \frac{C_{13}(C_{11} - C_{12})}{(C_{11}C_{33} - C_{13}^2)}$$

Taking the reference axes indicated in Figure 13.1, we obtain the following matrix {C}. The letter O indicates that outside of the diagonal and of the non-zero values of stiffness matrix components all the remaining terms are zero.

$$\{C\} \text{ (Pa)} \begin{pmatrix} 3.09 \times 10^{10} & 0.59 \times 10^{10} & 0.524 \times 10^{10} & & & \\ & 3.09 \times 10^{10} & 0.52 \times 10^{10} & & 0 & \\ & & 0.826 \times 10^{10} & & & \\ & & & 0.214 \times 10^{10} & & \\ & \text{Sym.} & & & 0.214 \times 10^{10} & \\ & & & & & 1.247 \times 10^{10} \end{pmatrix}$$

and also the following matrix {S}:

$$\{S\} \text{ (m}^2\text{/N)} \begin{pmatrix} 3.66 \times 10^{-11} & -3.5 \times 10^{-12} & -2.1 \times 10^{-11} & & & \\ & 3.66 \times 10^{-11} & -2.1 \times 10^{-11} & & 0 & \\ & & 1.47 \times 10^{-10} & & & \\ & & & 4.67 \times 10^{-10} & & \\ & \text{Sym.} & & & 4.67 \times 10^{-10} & \\ & & & & & 8.019 \times 10^{-11} \end{pmatrix}$$

Finally technical moduli of this material are :

$E_1 = E_2 = 27.3$ GPa, $E_3 = 6.8$ GPa, $G_{13} = G_{23} = 2.14$ GPa, $G_{12} = 12.4$ GPa

$\nu_{12} = \nu_{21} = 0.095$, $\nu_{13} = \nu_{23} = 0.57$, $\nu_{31} = \nu_{32} = 0.143$

13.6. List of symbols

13.6.1. *Latin alphabet*

E	Young's modulus
f	force
I	quadratic moment of the ring cross-section
l, m, n	roots of characteristic equation
N, T	normal and tangential force components
M	bending moment
M_r	ring mass
$m^2_c = -\frac{\mu}{E}\frac{f''}{f}$	ratio coefficient
p, q	coefficients in characteristic equation
$Q= m_c R^4/I$	coefficient in characteristic equation
R	mean radius of the ring
s	curvilinear coordinate

13.6.2. *Greek alphabet*

$\vec{\upsilon}$, $\vec{\tau}$, $\vec{\beta}$	Cartesian unit vector in polar coordinates
θ	angular displacement
μ	density
λ	variable in characteristic equation
ρ	Mass density
ζ , η	wave numbers
ω	angular displacement component

13.7. Bibliography

[BER 77] BERSEGOL J.P., Elastic and viscoelastic characteristics of pyrolitic graphite, Report of engineer final studies, in French, ISMCM, 93400, Saint-Ouen, France, 1977.

[CHE 10] CHEVALIER, Y. and VINH, J.T. (eds), *Mechanics of Viscoelastic Materials and Wave Dispersion*, ISTE Ltd, London, John Wiley and Sons, New York, USA, 2010.

[HOP 71] HOPPE R., "Vibrationeneines Ringes in seiner Ebene", *Journal für die reine und angewandte Mathematik (Crelle's),* Vol. 73, pp. 158–170, 1871.

[HAW 77] HAWKINGS D.L., "A generalized analysis of the vibration of circular rings", *Journal of Sound and Vibration,* Vol. 54, pp.67–74, 1977.

[KIR 71] KIRKHOPE J., "Vibration of system of elastically coupled concentric ring", *Journal of the Acoustical Society of America*, vol. 14, pp. 371–373, 1971.

[KUH 42] KUHL W., "Messungenzu den TheorienderEigenchwingungen von KreisringenbeliebigerWandstärke", *Akustische Zeitschrift*, Vol. 7, p. 125–152, 1942.

[LAM 88] LAMB H., *London Mathematical Society Proceedings*, Vol. 19, p. 165, 1888.

[LIN 67] LINCOLN J.W. & VOLTERRA E., "Experimental and theoretical determination of Frequencies of elastic toroids", *Experimental Mechanics*, vol. 24, pp. 211–217, 1967.

[LOV 34] LOVE A.E.H., *The Mathematical Theory of Elasticity*, Cambridge University Press, 1934.

[PHI 56] PHILIPSON L. L., "On the role of extension in the flexural vibrations of rings", *Journal of Applied Mechanics*, Vol. 23, pp. 324–336, 1956.

[RAO 69] RAOS. S. & SUNDARARAJAN V., In plane flexural vibration of circular ring, *Journal of Applied mechanics*, Vol. 91, pp. 620–625, 1969.

[SEI 64] SEIDEL B.S. & ERDELYI E.A., On the vibration of a thick ring in its own plane, *Journal of Engineering for Industry*, Vol. 86, pp. 240–243, 1964.

13.8. Appendix 13A. Evaluation of Young's modulus by using in plane bending motion of the ring

For a ring, a cylindrical coordinate is adopted. θ is the angle centered at the ring axis, u the coordinate along the radius, v the coordinate tangential to the ring in the ring plane. D'Alembert's principle enables the following equation of motion to be obtained (see Chapter 9 [CHE 10]):

$$\mu \left[\frac{\partial^4 v}{\partial \theta^2 \, \partial t^2} - \frac{\partial^2 v}{\partial t^2} \right] + \frac{EI}{R^4} \left[\frac{\partial^6 v}{\partial \theta^6} + 2\frac{\partial^4 v}{\partial \theta^4} + \frac{\partial^2 v}{\partial \theta^2} \right] = 0 \qquad [13.A.1]$$

where μ is the mass per unit length = ρS, ρ density, S the area of the cross-section, R ring radius, and I inertia moment of the ring cross-section.

The equation of the ring motion is of degree 6 compared to the degree 4 of the bending equation of the rod. If we use the separation variable method to find a solution of [13.A.1]:

$$s^6 + 2s^4 + s^2\left(1 - \frac{m^2R^4}{I}\right) + \frac{m^2R^4}{I} = 0 \qquad [13.A.2]$$

With $\lambda = s^2$ we obtain an equation of degree 3 in λ:

$$\lambda^3 + 2\lambda^2 + \lambda(1 - Q) + Q = 0 \qquad [13.A.3]$$

$Q = \frac{mR^4}{I}$ (where m is a positive integer), $\omega^2 = Em^2 / \mu$.

The successive steps to evaluate the solution are:

– evaluate the roots λ_i of [13.A.3];

– calculate Q_k[7] for each mode k;

– evaluate Young's modulus:

$$E = \frac{4\pi^2 f_k^2 \rho S R^4}{Q_k I} = \frac{2\pi f_k^2 R^3 M}{Q_k I} \qquad [13.A.4]$$

where M is the ring weight.

13.9. Appendix 13B. Determination of inertia moment of a solid by means of a three-string pendulum

13B.1. *Principle of the method*

An equilateral triangular horizontal plate is suspended by three strings of equal length. At rest, the strings are vertical (Figure 13B.1) where axis directions are indicated. H is the inertia center of the plate.

13B.1.1. *First measurement*

The eigenperiod of the plate submitted to a rotation around Hz is measured.

7 The eigenvalues Q_k must not be confused with Q in equation [13.A.3].

13B.1.2. *Inertia moment of the object*

The sample is put on the plate so as the object axis includes the inertia center and is coincident with axis Hz of the pendulum. The measurement of the period of the pendulum supporting the object is evaluated.

The two periods allow the calculation of the inertia moment of the object.

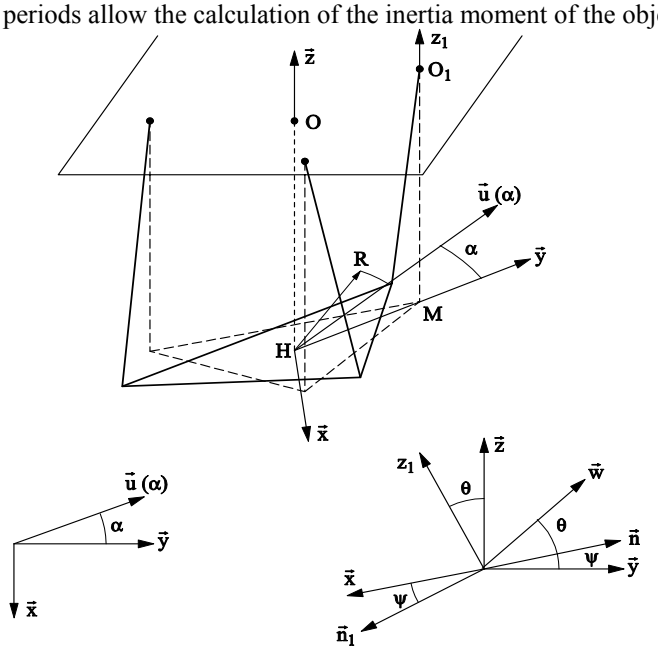

Figure 13B.1. *An equilateral triangle suspended by three strings is used to evaluate the inertia moment of an object put on a triangle platen. A vertical line containing the inertia center of the triangle coincides with axis H$\vec{z}$ of the object*

13B.2. *Calculations*

The following notations are adopted:

– m_0 plate mass

– m_1 object mass

– $m = m_0+m_1$

– R radius of the circle circumscribing the triangular plate

– L string length

– α, Θ, ψ angles indicated in Figure 13.B.1

– I_H inertia moment of the couple triangle-object

The rotations are the following:

$(\vec{x}, \vec{y}, \vec{z}) \rightarrow (\vec{v}, \vec{u}, \vec{z})$ rotation axis round $\vec{z}$, angle α

$(\vec{x}, \vec{y}, \vec{z}) \rightarrow (\vec{n}_1, \vec{n}, \vec{z})$ rotation axis round $\vec{z}$, angle ψ

$(\vec{n}_1, \vec{n}, \vec{z}) \rightarrow (\vec{n}_1, \vec{w}, \vec{z}_1)$ rotation axis round $\vec{n}_1$, angle θ

and then

$$\vec{u} = -\sin\alpha\ \vec{x} + \cos\alpha\ \vec{y}$$

$$\vec{z}_1 = -\sin\theta\ \sin\psi\ \vec{x} - \sin\theta\ \cos\psi\ \vec{y} + \cos\theta\ \vec{z}$$

We have:

$$\overrightarrow{OM} = -z\vec{z} + R\ \vec{u}\ (\alpha) \qquad [13.B.1]$$

$$\overrightarrow{OM} = R\vec{y} - L\overrightarrow{z_1} \qquad [13.B.2]$$

These two equations give:

$$\text{On}\ \vec{x}\ :\ -R\sin\alpha = -L\sin\theta\sin\psi \qquad [13.B.3]$$

$$\text{Ov}\ \vec{y}\ :\ R\cos\alpha = R + L\sin\theta\cos\psi \qquad [13.B.4]$$

$$\text{On}\ \vec{z}\ :\ -z = -L\cos\theta \qquad [13.B.5]$$

Let us designate F as string tension

$$\vec{s}\ (\text{string} \rightarrow s) = F\overrightarrow{z_1} \qquad [13.B.6]$$

$$\vec{z}.\overrightarrow{M_H}(\text{string} \rightarrow S) = \vec{z}\ [R\vec{u}\ (\alpha) \wedge F\overrightarrow{z_1}] \qquad [13.B.7]$$

$$\vec{z}\,\overrightarrow{M_H}(\text{string} \rightarrow S) = FR\sin\theta(\sin\alpha\cos\psi - \cos\alpha\ \sin\psi) = I_H\ \alpha'' \qquad [13.B.8]$$

[13.B.8] is the dynamic moment equation along axis $\vec{z}$.

The equation concerning the dynamic sum is:

$$-mz'' = -mg + F\cos\theta \qquad [13B.9]$$

Let us set: $L/R = \lambda$

Geometrical equations [13.B.3] to [13.B.5] give:

$$\left.\begin{aligned} &\sin\alpha = \lambda \sin\theta \sin\psi \\ &\cos\alpha = 1+\lambda\sin\theta\cos\psi \\ &z = L\cos\theta \end{aligned}\right\} \qquad [13.B.10]$$

α , θ being small, we obtain:

$$\left.\begin{aligned} &\alpha = \lambda\,\theta\sin\psi \\ &-\alpha^2/2 = \lambda\theta\cos\psi \\ &z = L(1-\theta^2/2) \end{aligned}\right\} \qquad [13.B.11]$$

From [13B.11] we deduce:

$$\tan\psi = -\frac{2}{\alpha} \quad , \quad \sin\psi = \frac{-2}{\sqrt{4+\alpha^2}} \quad , \quad \cos\psi = \frac{-\alpha}{\sqrt{4+\alpha^2}} \qquad [13.B.12]$$

$$\theta = [-\alpha/2\lambda]\sqrt{4+\alpha^2} \qquad [13.B.13]$$

$$L = z \quad \text{(first order approximation)} \qquad [13.B.14]$$

Equation [13.B.14] makes it possible to write [13.B.8] as follows:

$$mg = F \qquad [13.B.15]$$

Bringing [13.B.15] into [13.B.8] and retaining only first order terms:

$$I_H\,\alpha'' = -m\,g\,R\,\alpha/\lambda \qquad [13B.16]$$

This differential equation gives the period :

$$T = 2\pi\left[\, I_H\lambda / mgR \,\right]^{1/2} \quad \text{with} \quad \lambda / R \qquad [13.B.17]$$

Then I_H is deduced from [13.B.17]:

$$I_H = T^2[m_0\,g\,R / 4\pi^2\lambda] \qquad [13B.18]$$

The following notations are adopted:

I_0 , m_0 , T_0 inertia moment, weight, period of the platen alone;

I_1 , m_1 , T_1 inertia moment of the sample, weight of the sample, period of the set (sample + plate); see Figure 13B.1

From [13.B.18] the following equations are obtained:

$$\left.\begin{aligned} I_0 &= [\ T_1^2(m_0+m_1)gR] \,/\, 4\pi^2\lambda \\ (I_0+ I_1) &= [\ T_1^2(m_0+m_1)\ gR] \,/\, 4\pi^2\lambda \end{aligned}\right\} \qquad [13B.19]$$

I_1 is deduced from [13.B.19]:

$$I_1 = [(\ T_1^2 - T_0^2)\ m_0 + \ T_1^2\ m_1\ ]\ .\ gR \,/\, 4\pi^2\lambda \qquad [13B.20]$$

Inertia moment of the sample I_1 is obtained by measurements of the two periods T_0 , T_1

13.10. Appendix 13C. Necessary formulae to evaluate Young's modulus of a straight beam

A straight beam is presented in Figure 13.1 as sample A. However, the beam has a curved section. The inertia moment IG_0 must be calculated taking into account this section geometry, see equation [13.7].

As an elastic characterization of the graphite composite material is required, in the dynamic test we choose weak slenderness (ratio of thickness h to length l) and a low working frequency so that Bernoulli-Euler's equation is applicable.

$$EI\frac{\partial^4 w}{\partial x^4} + \rho S\frac{\partial^2 w}{\partial t^2} = 0 \qquad [13.C.1]$$

For simplification, we adopt in [13.C.1]:

$$I = I_{G\theta c}$$

As the sample is symmetric with respect to the sample middle and concerning the boundary conditions, i.e. pseudo-clamping in the middle and free ends at both side, we need therefore only examine half of the sample length l.

The natural boundary conditions are:

– at the free end, x=L:

bending moment M(L)=0 and shear force F(L)=0 [13.C.2a]

–at the free end: x=0:

displacement w(o) = 0 and slope $\frac{\partial w}{\partial x} = 0$ [13.C.2b]

To find a closed form expression of the boundary equations, characteristic functions are referred to:

$$w(x,t) = e^{j\omega t}\left[A\ \sin\frac{\beta x}{L} + B\cos\frac{\beta x}{L} + C\ \sinh\frac{\beta x}{L} + D\cosh\frac{\beta x}{L} \right] \qquad [13.C.3]$$

The four boundary conditions [13.C.2] permit the set of coefficients A, B, C, D to be evaluated.

Finally the eigenequation for the clamped free rod is:

$$1+\cos\beta\ \cosh\beta = 0 \qquad [13.C.4]$$

The first eigenvalues are given in [13.10d].